25th IMEKO TC4 International Symposium
23rd International Workshop on ADC and DAC Modelling and Testing
IMEKO TC-4 2022
Brescia, Italy / September 12-14, 2022

A Preliminary Study on Flexible Temperature Sensors for Eskin Medical Devices

Fapanni Tiziano[1], Emilio Sardini[1], Mauro Serpelloni[1]

[1]*University of Brescia, Brescia, Italy, {t.fapanni, emilio.sardini, mauro.serpelloni}@unibs.it*

***Abstract* – In the latest years, the need of a renewed paradigm for healthcare arose promoting the research towards the idea of remote diagnosis, care and monitoring of physiological parameters. Thus, the wearable and eskin devices arose to be embedded in the standard medical equipment. In this work, a preliminary study on flexible AJP-printed temperature sensors is reported in order to propose a novel approach to evaluate infection sites, monitor the body temperature and compensate the effects of temperature on other on-body sensors. Two different geometries are proposed, designed, produced, evaluated and compared. The results shown a similar dependance on temperature (average TCR = $2.5 \cdot 10^{-3}$ °C^{-1}) and the dependance on substrate deformation was enquired as well as the geometrical features of the sensors.**

I. INTRODUCTION

In the latest years, the need of a renewed paradigm for healthcare arose. The idea of remote diagnosis, care and in general of physiological parameters monitoring is appealing [1]. To address this arising need, new technology arose in the latest years trying to miniaturize the standard medical equipment to fit it in a wearable device [2]. Wearable devices are now widespread both for selfcare monitoring, sports medicine, diagnostics, prosthetics and feedback treatment for rehabilitation [3]–[5]. At the state of art, most wearable devices are wrist watches or bands that provide lower-quality signal collection than the ones that could be collected by skin-like devices [6]. Those devices can be called eskins devices and can be defined as large area and flexible devices that can cover part of the human body mimicking the skin. Those embeds different sensors to collect information both from the environment end from the body itself [7]–[11]. To produce those devices different techniques have been explored in the literature including both classical techniques of microfabrication (e.g. chemical vapor deposition, sputtering, photolithography, etc.) and printed techniques. The latter provide a quicker prototyping process, offers a wide set of different materials and can be adapted to work even on non-planar surfaces. Among the possible printed techniques, aerosol jet printing (AJP) was selected for this preliminary study thanks to its flexibility in terms of available viscosity of the inks and its fully digital and maskless production process. Thus, this technique allows a quick and cheap prototyping that is ideal in the research frame. AJP basic principles are already described in literature [12]. Briefly, three flows of gases are used to atomize the ink (atomizer flow), control the dimension of the particles (exhaust flow) and to focus the aerosol on the nozzle (sheath flow). The eskin sensors cover a plethora of applications such as force sensing, humidity detection, temperature, strain/twist, limb bending, biopotentials and biomarkers. Temperature sensors are of particular interest in the medical field such as for infective diseases and illness control [13]–[15]. Moreover, temperature is a common influence variable for other sensors such as strain gauges and electrochemical sensors [16], [17]. Thus, monitoring the temperature on site and real time can help to compensate its effects on other sensors to obtain reliable information. In the literature different kind of temperature sensors are reported, each featuring its pros and cons. Positive and Negative temperature coefficient thermistors (PTC and NTC respectively) as well as integrated temperature sensors are rigid and usually employ non-printable materials. Thermocouples require to know the temperature at the reference junction and therefore this is not feasible in many wearable applications. On the other hand, resistive temperature sensors (RTD) use the thermoresistive effect of metals allowing simple geometry designs and a production process compatible with printed electronics. Thus, among the different typologies of temperature sensors, RTDs are the most suitable for a fully printed, compact and flexible design. Flexibility, however, may vary the resistance of the sensor due to the effects of deformation of the substrate. Thus, the aim of this work is to propose a preliminary study on flexible AJP-printed temperature sensors. The proposed printed sensors will be characterized analyzing their geometry and the effects of substrate deformation.

II. MATERIALS AND METHODS

The design process of the sensor started analyzing different possible geometries. Among the possible the ones in Fig. 1 where selected. A standard strain gauge-like geometry (Fig. 1a) was selected as state of art and designed following commercial strain gauges. On the other hand, a double helix geometry was further proposed to reduce the area of the sensor and uniform the dependance on strain in

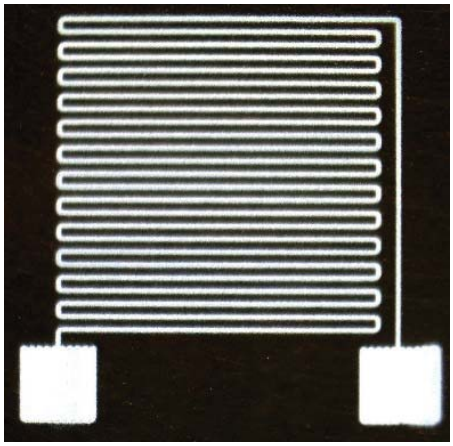

(a)

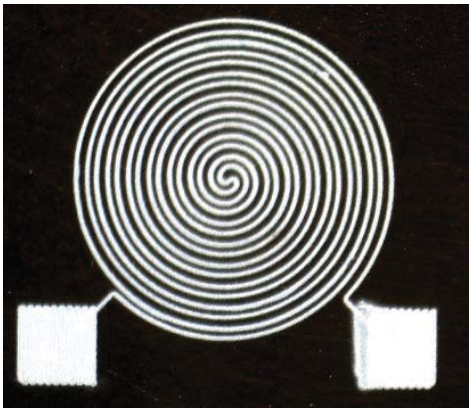

(b)

Fig. 1. Microscope images of the different geometries evaluated in this work. A standard strain gauge geometry (a) and the proposed double helix (b)

each direction. Both the geometries were designed with similar length and with target linewidth of 150 μm.

The devices were printed on a flexible polimide foil (Kapton, DuPont de Nemours, Luxembourg, Grand Duchy of Luxembourg) using an Aerosol Jet Printer (AJ300, Optomec, Albuquerque, NM, USA). The substrate was selected considering the most common substrates used for eskins as well as the mechanical and electrical proprieties of the available materials [18]. Among the possible inks, a silver ink (Smart Aero, Genesink, Rousset, France) was selected and deposed after cleaning the substrate with ethanol to increase the ink-substrate adhesion. The selected process parameters were 1240 SCCM for the sheath flow, 850 SCCM for the atomizer flow and 800 SCCM for the exhaust flow with a process speed of 3 mm/s. The ink was thermally cured in an oven at 150 °C for 60 minutes according to the producers' specifications to achieve proper electrical conductivity.

A. Process Evaluation

In order to evaluate the outcome of the production process two sets of evaluations were carried on. At first, the sensors were inspected using an optical microscope NB50T (Orma Scientific, Sesto San Giovanni, Milan, Italy) equipped with a trinocular zoom 0.8x–5x–LED and a camera. In this evaluation step the lines were analyzed and measured. Then a Filmetrics Profilm 3D optical profilometer (Filmetrics Inc., 10655 Roselle St., San Diego, CA, USA) was used to evaluate the thickness of the printed features.

B. Resistivity Evaluation

In order to calculate the average resistivity (ρ), a set of three straight, 2 cm-long lines were printed. The resistivity (ρ) was then calculated using equation 1 where l is the length (known by design), R is the measured resistance and S is the average cross-section area of the conductor. This was evaluated through the optical profilometer, measuring the profile in three different positions for each sample.

$$\rho = R \cdot \frac{S}{l} \tag{1}$$

The resistance was evaluated using a digital bench-top multimeter Hewlett–Packard 34401a (HP, Palo Alto, CA, USA) and a 4-wire technique.

C. Sensitivity to Substrate Bending

To evaluate the differences between the two geometries different features were evaluated. The behavior of the two geometries under deformation was evaluated. Briefly, the sensors were placed on a planar substrate, then they were bended onto a cylinder with radius 30 mm. The selected deformation axis was the one that maximized the sensibility of the devices. The variation in resistance is measured by a multimeter Hewlett–Packard 34401a with a 4-wire technique. One sample for each geometry was analyzed in bending.

D. Sensitivity to Temperature Variations

In order to evaluate the behavior of the sensors in relation with the temperature they were placed on top of an hotplate and covered with a beaker to avoid airflows. A pt100 was mounted nearby to provide a reliable measurement of the temperature applied to the sensors. All the measurements of resistance were performed using a 4-wire technique with a set of the aforementioned Hewlett–Packard 34401a multimeters connected with a computer through a GPIB interface and controlled by a LabVIEW interface that samples the signals at 1 Hz.

At first a set of increasing temperature setpoints

ranging from room temperature up to 80°C were imposed each for 20 minutes. Then the hotplate was switched off and left to cool down back to room temperature. The collected data were then analyzed in MATLAB to obtain the temperature coefficient of resistance (TCR, α in the equation) and the resistance at 0°C (R_0) to be used in the calibration relation shown in equation 2.

$$R = R_0 \cdot (1 + \alpha T) \quad (2)$$

III. RESULTS AND DISCUSSION

A. Process Evaluation

The microscope evaluation aimed to measure the average line width and its variations in the production process. On the double helix geometry, the width was evaluated as (137 ±19) µm, while it resulted (157 ±16) µm for the strain gauge geometry. In the latter a smaller standard deviation was achieved due to the use of straight lines. In fact, straight lines are a simple trajectory that is easier to produce with linear stepper motors employed by the AJP. The analysis at the optical profilometer provided a set of clear images on the thickness of the printed traces revealing an uneven deposition of the functional material and an average thickness of 0.6 µm for the double helix and 0.4 µm for the classical strain gauge geometry.

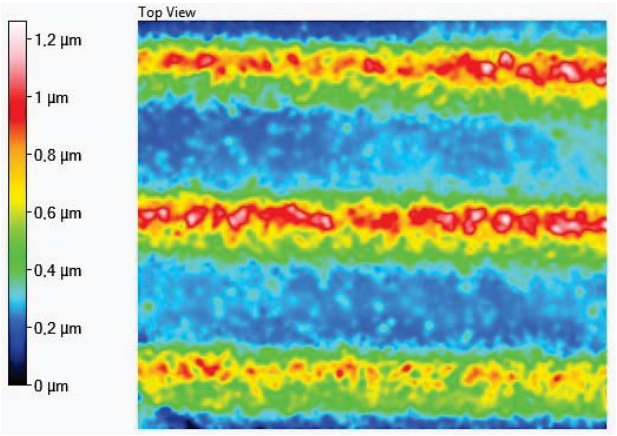

(a)

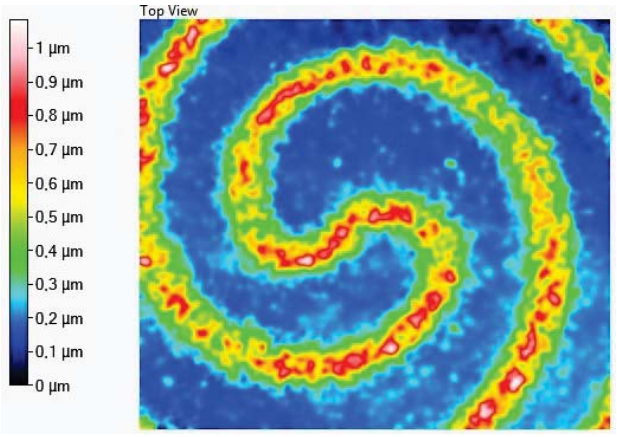

(b)

Fig. 2. Thickness of the printed lines obtained for the standard strain gauge geometry (a) and for the proposed double helix (b)

B. Resistivity Evaluation

The average line width for the straight lines used for the resistivity evaluation resulted (52.3±4.5) µm. The average cross-section area was evaluated by integrating the data collected with the optical profilometer through a MATLAB program. An average of (150.3±30.0) µm^2 was obtained. The measured line-resistance resulted on average (10.90±4.85) Ω. The obtained average resistivity resulted (8.2±4.0) Ωcm that resulted comparable with the one presented in the ink datasheet.

C. Sensitivity to Substrate Bending

The resistance variation due to substrate deformation is shown in Fig. 3. The two geometries presented a slightly different behavior when subjected to the same stimulus. The double helix geometry (in blue in the image) presented a fast-rising spike that settled then to a lover value and has equally fast rising and falling times. On the other hand, the strain gauge geometry (in red in the image) presented a slower rising and falling times similar to a first order system behavior. Both the geometries however presented a small variation of the resistance evaluated in the rest position.

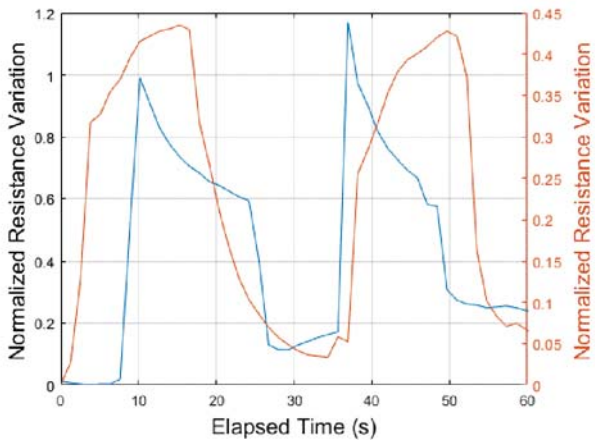

Fig. 3. Stress-induced resistance variation in the sensors for double helix (blue) and strain gauge (red) geometries

D. Sensitivity to Temperature Variations

The relative variations of sensors resistance to temperature are shown in Fig. 4. The printed devices present similar behavior perfectly comparable to the one of the Pt100 used as reference sensor. Moreover, the collected data was used to obtain a resistance-temperature

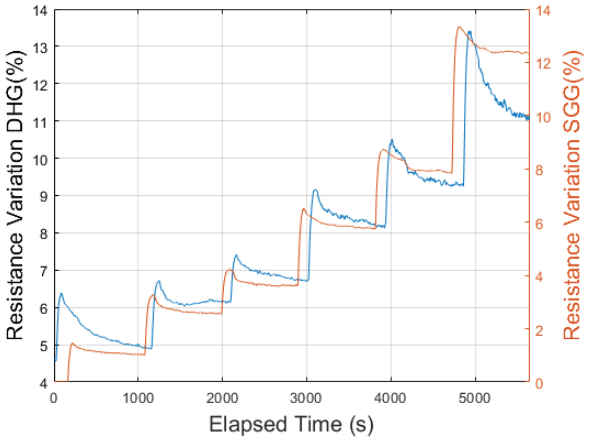

Fig. 4. Temperature dependance of the sensors shown in time. The resistance variation for the double helix geometry is reported in blue, while the one of the strain gauge geometry is reported in red

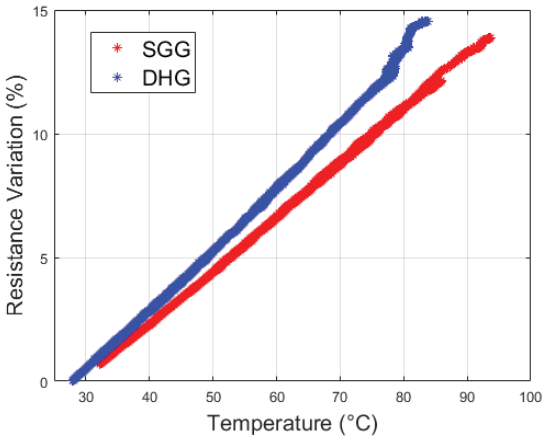

Fig. 5. Resistance-Temperature plot for the strain gauge geometry (in red) and the double helix geometry (in blue)

characteristics for each sensor (Fig. 5). Both resulted linear, with reduced hysteresis. As regards the sensibility, the double helix geometry performed slightly better with a TCR of $2.7\pm0.3\cdot10^{-3}$ °C^{-1} than the strain gauge geometry (TCR=$2.3\pm0.1\cdot10^{-3}$ °C^{-1}).

IV. CONCLUSIONS

In this work, two different geometries were preliminary analyzed in order to propose a fully AJP printed and flexible temperature sensor that can be used in the eskin application field. The sensors were designed and produced. Then the production process, the design idea and the materials were evaluated. The average resistivity of the conductive ink was evaluated to be 8.2 Ωcm and comparable with the one presented in the material datasheet. Microscope analysis provided an average line width of 137 µm for the double helix geometry and 157 µm for the strain gauge one. A preliminary evaluation of the resistance variation under deformation was performed and revealed that the two geometries perform in different way, but the double helix presented lower variations. Considering on the other hand the effects of temperature, the two geometries performed similarly and resulted linear, with reduced hysteresis and similar sensibility. Even though, those results are promising, different future research topics are still open, such as exploring different materials and new geometries, as well as designing a whole system whose metrological characteristics can meet application requirements, such as a temperature resolution of 0.1°C.

REFERENCES

[1] S. Zhang, S. Li, Z. Xia, and K. Cai, "A review of electronic skin: Soft electronics and sensors for human health," *J. Mater. Chem. B*, vol. 8, no. 5, pp. 852–862, 2020, doi: 10.1039/c9tb02531f.

[2] K. K. Yeung, T. Huang, Y. Hua, K. Zhang, M. M. F. Yuen, and Z. Gao, "Recent Advances in Electrochemical Sensors for Wearable Sweat Monitoring: A Review," *IEEE Sens. J.*, vol. 21, no. 13, pp. 14522–14539, 2021, doi: 10.1109/JSEN.2021.3074311.

[3] A. C. Bunea *et al.*, "E-skin: The dawn of a new era of on-body monitoring systems," *Micromachines*, vol. 12, no. 9, 2021, doi: 10.3390/mi12091091.

[4] E. Cantu *et al.*, "Printed Multi-EMG Electrodes on the 3D Surface of an Orthosis for Rehabilitation: A Feasibility Study," *IEEE Sens. J.*, vol. 21, no. 13, pp. 14407–14417, 2021, doi: 10.1109/JSEN.2021.3059308.

[5] S. Tonello *et al.*, "Preliminary study of a flexible printed multi-sensing platform for electromyography and lactate measuring during rehabilitation," *2021 IEEE Int. Symp. Med. Meas. Appl. MeMeA 2021 - Conf. Proc.*, 2021, doi: 10.1109/MeMeA52024.2021.9478729.

[6] H. S. Oh, C. H. Lee, N. K. Kim, T. An, and G. H. Kim, "Review: Sensors for biosignal/health monitoring in electronic skin," *Polymers (Basel).*, vol. 13, no. 15, 2021, doi: 10.3390/polym13152478.

[7] J. Huang *et al.*, "Editors' Choice—Review—Impedance Response of Porous Electrodes: Theoretical Framework, Physical Models and Applications," *J. Electrochem. Soc.*, vol. 167, no.

16, p. 166503, 2020, doi: 10.1149/1945-7111/abc655.

[8] G. Wolterink, R. Sanders, F. Muijzer, B. van Beijnum, and G. Krijnen, “3D-printing soft sEMG sensing structures,” in *2017 IEEE SENSORS*, 2017, pp. 1–3, doi: 10.1109/ICSENS.2017.8233935.

[9] K. Kim *et al.*, “Low-voltage, high-sensitivity and high-reliability bimodal sensor array with fully inkjet-printed flexible conducting electrode for low power consumption electronic skin,” *Nano Energy*, vol. 41, no. June, pp. 301–307, 2017, doi: 10.1016/j.nanoen.2017.09.024.

[10] P. S. Das and J. Y. Park, “A flexible touch sensor based on conductive elastomer for biopotential monitoring applications,” *Biomed. Signal Process. Control*, vol. 33, pp. 72–82, 2017, doi: 10.1016/j.bspc.2016.11.008.

[11] M. Chung, G. Fortunato, and N. Radacsi, “Wearable flexible sweat sensors for healthcare monitoring: A review,” *J. R. Soc. Interface*, vol. 16, no. 159, 2019, doi: 10.1098/rsif.2019.0217.

[12] M. Borghetti, E. Cantù, E. Sardini, and M. Serpelloni, “Future sensors for smart objects by printing technologies in Industry 4.0 scenario,” *Energies*, vol. 13, no. 22, 2020, doi: 10.3390/en13225916.

[13] H. S. Jeon, J. H. Kim, M. B. G. Jun, and Y. H. Jeong, “Fabrication of thermochromic membrane and its characteristics for fever detection,” *Materials (Basel).*, vol. 14, no. 13, 2021, doi: 10.3390/ma14133460.

[14] Y. Zhang *et al.*, “Flexible integrated sensing platform for monitoring wound temperature and predicting infection,” *Microb. Biotechnol.*, vol. 14, no. 4, pp. 1566–1579, 2021, doi: 10.1111/1751-7915.13821.

[15] A. Al-Halhouli, A. Albagdady, J. Alawadi, and M. A. Abeeleh, “Monitoring symptoms of infectious diseases: Perspectives for printed wearable sensors,” *Micromachines*, vol. 12, no. 6, pp. 1–35, 2021, doi: 10.3390/mi12060620.

[16] S. Yoon, H. Yoon, M. A. Zahed, C. Park, D. Kim, and J. Y. Park, “Multifunctional hybrid skin patch for wearable smart healthcare applications,” *Biosens. Bioelectron.*, vol. 196, no. October 2021, p. 113685, 2022, doi: 10.1016/j.bios.2021.113685.

[17] Y. Zhao, Y. Liu, Y. Li, and Q. Hao, “Development and application of resistance strain force sensors,” *Sensors (Switzerland)*, vol. 20, no. 20, pp. 1–18, 2020, doi: 10.3390/s20205826.

[18] Z. Yuan, S. T. Han, W. Gao, and C. Pan, “Flexible and Stretchable Strategies for Electronic Skins: Materials, Structure, and Integration,” *ACS Appl. Electron. Mater.*, vol. 4, no. 1, pp. 1–26, 2022, doi: 10.1021/acsaelm.1c00025.